Jefferson Lab

Newport News, VA

GlueX/Hall D Calorimeter Final Design and Safety Review
February 19-20, 2008

Section 4:
FCAL – The Forward Calorimeter

GlueX/Hall D Calorimeter Conceptual Design Report
Section 4 of 5

4 FCAL: The Forward Calorimeter

4.1 Overview

The cylindrical barrel calorimeter (BCAL) and the planar forward calorimeter (FCAL) complement each other in carrying out photon detection for the GlueX detector. The FCAL is a 2.4 m diameter circular stack of 2800 lead glass blocks (see Figure 4.1) whose front face is located 560 cm downstream of the GlueX target center.

The glass, manufactured in Russia, is designated as type F8-00 glass with a chemical composition of 45% PbO, 42.8% SiO_2, 10.4% K_2O and 1.8% Na_2O. The glass has a density of 3.6 g/cm^3, a radiation length of 3.1 cm, a nuclear collision length of 22.5 cm and an index of refraction of 1.62. The Molière radius of the glass is 4.3 cm. The lead glass blocks have transverse dimensions of 4×4 cm^2 (within 50 microns in each transverse dimension) and are 45 cm long. Each block is optically isolated from the others by an aluminized mylar wrapping. The center 3×3 blocks are removed to produce a 12×12 cm^2 beam hole.

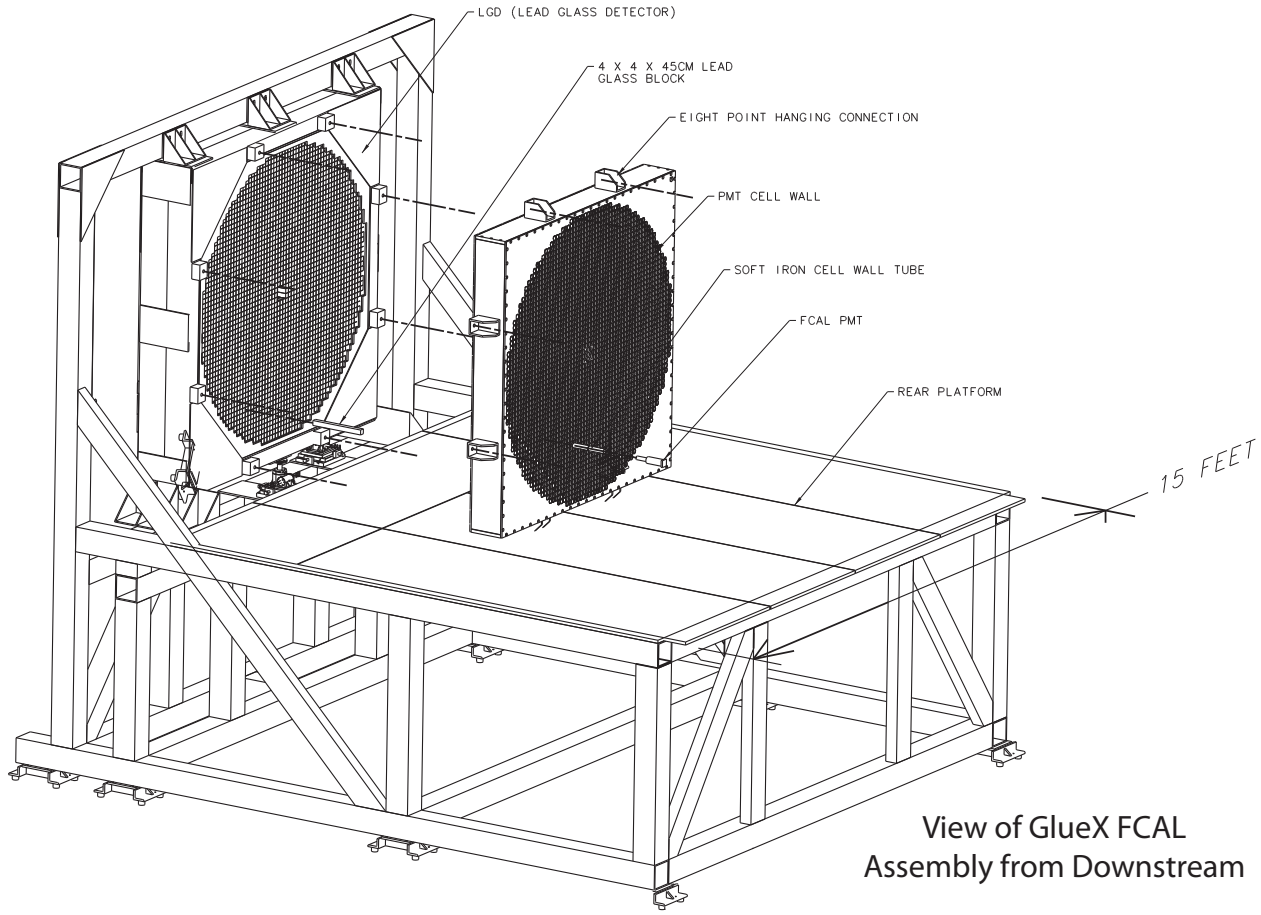

Figure 4.1: The forward calorimeter (FCAL) consisting of 2800 lead glass blocks arranged in a circular stack. The front of the array is located 560 cm downstream of the target center. The diameter of the circular stack is 240 cm.

Each block will be read out using a FEU 84-3 photomultiplier tube (PMT), also manufactured in Russia. These twelve-stage PMTs have a maximum gain of 2.4×10^5. The 2.5 cm diameter borosilicate photocathode is sensitive to wavelengths between 300 and 820 nm. The quantum efficiency peaks at a wavelength of 400 nm with a value of about 24%. The PMT has a physical length of about 11 cm and a diameter of 3 cm. The PMTs will be powered by custom-designed Cockcroft-Walton bases [1]. An important feature of the Cockcroft-Walton bases is their relatively low power dissipation – about 0.2 W per base.

4.2 Guidance from E852 and RadPhi

The design of the FCAL largely makes use of the experience gained in constructing and operating very similar lead glass calorimeters for the E852 experiment at Brookhaven and the RadPhi experiment in Hall B at JLab. We begin by briefly reviewing the E852 and RadPhi experiences with particular emphasis on the details pertinent to the GlueX design.

The E852 experiment[2] studied $\pi^- p$ interactions at 18 GeV/c. In the E852 experiment the lead glass calorimeter was a rectangular array of 3045 blocks [3, 4] located about 5 m downstream of the production target in the Brookhaven Multiparticle Spectrometer (MPS). The MPS included tracking chambers inside a dipole magnet with a central field of 1 T. The calorimeter was used with a neutral final state trigger to study the final states $\pi^0\pi^0 n$ [5] and $\eta\pi^0 n$ [6]. Final states with charged particles and photons were also studied and these included final states such as $\pi^-\pi^0\pi^0 p$ [7], $\omega\eta n$ [8], $\eta\eta\pi^- p$ and $\eta\omega\pi^- p$ [9], among others. In E852 the photon positions on the face of the lead glass array were measured with a position resolution of $\sigma_r \approx 5-6$ mm. The energy resolution was given by $\sigma_E/E(\%) = 5.2/\sqrt{E(\mathrm{GeV})} + 2.0$. The energy of the lowest energy reconstructed photons was $\sim 120-150$ MeV.

The lead glass array in the RadPhi experiment was an approximately circular stack of 620 blocks with a 8×8 cm^2 central beam hole. The calorimeter was used in the tagged photon beam downstream of the CLAS detector in Hall B. The bremsstrahlung photon beam was produced using a 5.65 GeV electron beam. The total photon rate within the tagging range between 4.38 and 5.38 GeV was 5×10^7 per second, a factor of five larger than planned for initial GlueX running and a factor of two lower than planned for higher rate running. The RadPhi experience of operating an electromagnetic calorimeter in a high intensity photon beam is extremely valuable as it represents an environment very similar to what is expected in GlueX. In RadPhi the photon positions on the face of the lead glass array were measured with a position resolution of $\sigma_r = 6.4/\sqrt{E(\mathrm{GeV})}$ mm and energy resolution was given by $\sigma_E/E(\%) = 7.3/\sqrt{E(\mathrm{GeV})} + 3.5$.[1]

The calorimeters in both the E852 and RadPhi experiments used a gain monitoring system based on a pulsed nitrogen laser that illuminated a 1 cm^3 cube of plastic scintillator. The light from this scintillator was delivered via fibers to the edges of a sheet of Plexiglas covering the upstream face of the array. Most of the light is trapped by total internal reflection but enough light escapes to provide a sufficiently uniform illumination of the lead glass array. A similar arrangement is planned for GlueX.

Based on the experience, primarily from RadPhi, there are several issues that require careful attention in developing the optimal forward calorimeter design for GlueX. We highlight these in detail below.

[1] It is difficult to isolate the source of the apparent discrepancy between E852 and RadPhi resolutions. It should be noted that the techniques for obtaining these resolutions and the energy ranges over which they are studied are different for the two experiments. As RadPhi is most similar to the final GlueX design, we take it as the best estimator for GlueX resolution.

4.2.1 PMT optical coupling

Simulations were performed to interpret data from the RadPhi calorimeter, in particular to take into account the presence of the a small gap at the interface between the block and the phototube [10]. One consequence of the gap is that light emitted at the critical Čerenkov angle of 52° by a particle moving parallel to the block axis has zero probability of being detected at the phototube; these photons are entirely contained inside the block by total internal reflection.

Two important consequences follow from this observation. The first is that the overall shower response goes through a local minimum at normal incidence, where a large fraction of the shower particles are in the "blind spot", with radiating shower particles nearly parallel to the block axis. The simulation showed that at 20° the light output from a 1 GeV shower was about 20% greater than at normal incidence. The second consequence is that the observed lateral size of a shower must be larger than the size expected based upon the shower energy deposition profile. This follows from the fact that the most energetic particles in a shower are found near the center of the shower profile and these are the particles whose directions are most likely parallel to the block axis. The observed light yield coming from the core of the shower distribution is thus suppressed relative to light coming from the shower periphery where particle energies are lower and directions are more random. In fact, there was a discrepancy of nearly 50% between observed shower size in RadPhi data and Monte Carlo before this angle-dependent collection efficiency was understood. After the effect was included in the simulation, the shapes of real and simulated showers were compared in terms of spatial moments up to the fourth moment and they were found to be in agreement within measurement errors.

The air gap between the lead glass block and the PMT also, in general, results in reduced efficiency for collecting Čerenkov photons and therefore poorer energy resolution and sensitivity to low energy showers. An added complication exists in the GlueX case in that the area around the FCAL is expected to be be immersed in a substantial fringe field (≈200 G) from the solenoid. Any mechanism of optically connecting the PMT to the lead glass must also provide magnetic shielding for the sensitive photocathode.

4.2.2 Electromagnetic backgrounds and radiation damage

Online monitoring of the RadPhi calorimeter during the experiment [10] indicated that the gain in the eight blocks immediately adjacent to the beam hole decreased as the run progressed. This observation was based upon the laser monitor system, the raw pulse-height distributions, and the channel gains which were periodically determined during the run. A similar effect was seen, but to a lesser degree, for the next ring of blocks once removed from the beam hole.

During a pause in the experiment, visual inspection of the blocks indicated that the glass was darkening, a well- known effect of radiation damage on lead glass. Figure 4.2 illustrates the gain reduction with beam time (roughly proportional to integrated radiation dose) for a typical block adjacent to the beam hole. It is apparent that the gain change is a gradual, cumulative effect rather than a sudden change which might be characteristic of a beam mis-steering event.

The magnitude of the gain loss (≈ 35%) was such that it could be compensated by adjustments of the PMT high voltages. This was done periodically during the experiment. The last datum in Figure 4.2 shows the result of one adjustment. However, this is only a partial solution, since a radiation damaged block produces fewer photo- electrons in the PMT, resulting in a degraded energy resolution which cannot be compensated

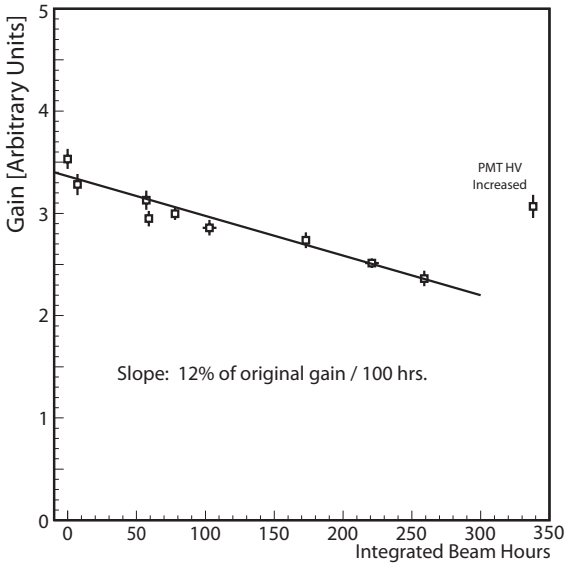

Figure 4.2: The effect of radiation damage on the central part of the detector. The last point shows the gain improvement after an adjustment of the phototube high voltage.

by increasing the PMT gain.

It is expected that the radiation environment in GlueX will be comparable to RadPhi. Not only will this present the problem of significant radiation damage to the inner calorimeter blocks, it will also result in an high rate for spurious electromagnetic showers in the calorimeter that must be appropriately handled at the analysis stage. Solutions to both of these issues in the form of radiation-hard blocks and advanced readout electronics will be presented.

To summarize, we proceed with a design for the GlueX calorimeter that is very similar to that employed in both E852 and RadPhi. Additional design modifications are needed to optimize the optical connection between lead glass blocks and PMTs while meeting magnetic shielding requirements and to ensure the calorimeter performs well in the high-rate GlueX photon beam.

4.3 Hardware assessment

In the sections below we summarize the status of the existing FCAL hardware. The lead glass, PMTs, and signal cables have been recycled from E852 and RadPhi. In order to build the GlueX FCAL, we plan to design and construct a new glass and PMT holding structure, a different PMT optical coupling, and new PMT bases. In addition we will be using a different electronics readout configuration: flash ADCs instead of conventional charge-integrating ADCs.

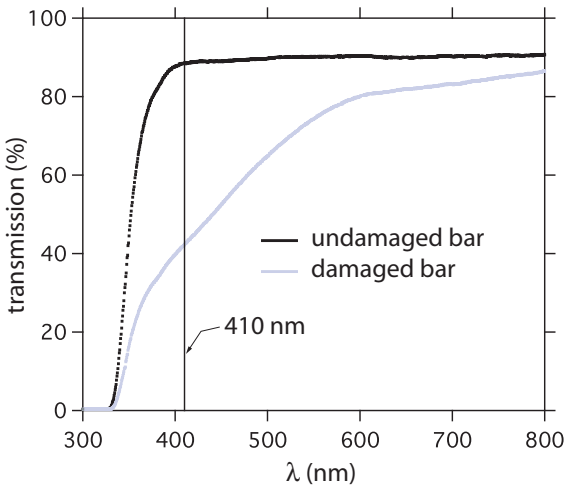

Figure 4.3: Transmission of light through 4 cm of lead glass for an undamaged bar and a radiation damaged bar as a function of wavelength.

4.3.1 Lead glass evaluation

As a result of use in E852 and RadPhi a number of the blocks had visible radiation damage. Radiation damaged blocks can be restored to the original pristine condition by heat treating. All lead glass blocks were inspected and those with notable damage were treated. We outline the procedure below.

Lead glass transmission measurements: The transmission of the lead glass bars was measured as a function of wavelength (λ) using a Shimadzu Model UV-160 spectrophotometer. The light from the spectrophotometer was transmitted through the 4 cm dimension of the block. Figure 4.3 shows the fraction of light transmitted as a function of wavelength for a typical F8-00 lead glass bar that had not been exposed to radiation above normal background. The transmission recorded by the spectrophotometer is not corrected for losses due to reflections. Ignoring any absorption of light in the glass, the fraction transmitted accounting for reflections at two surfaces should be $(4n/(n+1)^2)^2$ or 89.1% for $n = 1.62$. The average measured transmission for the undamaged bar for λ between 500 and 800 nm is $89.1 \pm 0.1\%$.

Also shown in Figure 4.3 is the transmission of a bar that had visible yellowing due to radiation damage. In subsequent measurements of the transmission, before and after heat curing, we measured the the transmission of light through the bars at $\lambda = 410$ nm where the transmission of undamaged bars has plateaued and where the relative difference between damaged and undamaged bars is typically large. The absolute quantum efficiency of the Russian FEU 84-3 phototubes used with these lead glass bars also peaks at this wavelength [3]. The Shimadzu spectrophotometer was modified to accommodate the full length of the lead glass bars to allow for measurements of the transmission of light at fixed wavelength for positions along the entire length of the bar.

Heat curing technique: An important issue with heat curing was to avoid cracking of bars due to thermal stresses caused by non-uniform heating or varying the temperature too quickly. We constructed an aluminum box that could accommodate two lead glass bars and sufficient lime powder, acting as a thermal mass, to completely surround each bar with at least 2.5 cm of powder. A temperature probe was also placed inside the box. Two household-grade stove ovens were used with a maximum temperature of 260 °C (500 °F). During production curing two aluminum boxes were inserted in each oven with each box holding two bars. Each oven was set at its maximum temperature setting. With the oven setting at 260 °C, the temperature of thermal mass surrounding the glass reaches 90% of its maximum temperature within approximately 3 hr.

The bars cured at the maximum temperature for at least 12 hr and the bars were allowed to cool for at least 3 hr before being removed from the aluminum boxes. During production, bar were heat cured at the rate of eight per day. A total of 600 bars were treated.

Figure 4.4 shows the transmission of light, at $\lambda = 410$ nm, through 4 cm of lead glass as a function of distance along the bar for a radiation-damaged bar before and after heat curing at 260 °C. The $z = 0$ position corresponds to the upstream end of the bar during data taking, *i.e.* the end of the bar closest to the source of the photon beam.

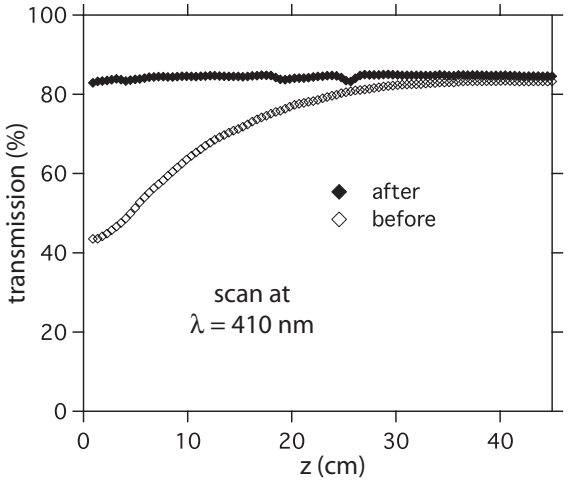

Figure 4.4: Transmission of light, at $\lambda = 410$ nm, through 4 cm of lead glass as a function of distance along the bar for a radiation-damaged bar before and after heat curing at 260 °C.

The heat curing technique restores the transmission properties of the lead glass bars to their state before suffering radiation damage. The transmission characteristics of each of the 600 treated bars was recorded before and after heat curing to ensure repair of damage. The net result is that approximately 2900 blocks are available for use in the FCAL. We anticipate a need of about 2700 blocks[2]; therefore, there is a comfortable spare margin to complete construction.

4.3.2 PMT evaluation

Each of the FEU 84-3 PMTs that were used in both E852 and RadPhi have been inspected and tested under high-voltage in a dark environment with an LED light source. For those PMTs that were not visibly

[2]There are 2800 blocks in the full array; however, we plan to instrument the center with radiation-hard blocks, as discussed in more detail later.

damaged there appeared to be no degradation in performance. By the time that the PMTs are installed and operated in GlueX they will be approximately 25 years old; however, there is no evidence that this is an unrealistic lifetime for FEU 84-3 PMTs. There are several examples of FEU 84-3 longevity: GAMS-4000 with 4000 FEU 84-3 was constructed in 1980 and used in NA-12, NA-12/A, WA-102 experiments at CERN and now in COMPASS; and GAMS-2000 with 2000 FEU 84-3 constructed at the end of 1970s is used now in OKA experiment at IHEP. In total we have approximately 2750 PMTs and plan to procure an additional 800 so that we have suitable spares to successfully operate the GlueX FCAL.

4.3.3 Signal cable refurbishment

The cables that we intend to use for GlueX readout are the refurbished E852 signal cables. Of the 3000 E852 cables, 2500 have already been cut to the appropriate length, had a new connector installed on one end, and have been tested. An additional 300 cables will be refurbished during GlueX construction.

4.4 GlueX design modifications

We now focus on the specific items identified from our RadPhi and E852 experience that need to be addressed in order to guarantee successful construction and operation of GlueX FCAL, namely, an improved PMT optical coupling that meets magnetic shielding requirements and method to handle backgrounds and radiation damage associated with an intense photon beam.

4.4.1 PMT optical coupling

In order to maximize resolution of the calorimeter, one needs an efficient optical connection from the lead glass bar to the PMT. This problem is complicated by the fringe field from the GlueX solenoid in the region of the calorimeter, which is expected to be on the order of 200 Gauss. This requires soft iron shielding of a few millimeter thickness around the PMT in addition to μ-Metal shielding. This shielding needs to extend beyond the photo-cathode by at least 3 cm (the diameter of the PMT) or more. Therefore the PMT can not be coupled directly to the lead glass block and a light guide is required between the PMT and the lead glass as shown in Figure 4.6.

Light guide design: In developing a design for the light guide, it is important to consider the unique angular distribution of Čerenkov photons as they strike the back of the block (shown in Figure 4.5). Increasing the index of refraction of the interface between the glass block and PMT reduces total internal reflection that traps light inside of the block and increases light collection efficiency. The choice of the best geometric form for the light guide is based on Monte Carlo simulations [11] and a cost vs. performance optimization. A suitable, easy-to-machine choice of material is UV transparent Plexiglas. Using a MC simulation based on a Geant4 modeling of the surface properties of the lead glass block, the light guide geometry and the optical coupling between the two and the PMT was studied. It was shown that using a simple cylindrical form was nearly as effective as more complicated Winston cone designs [11]. This is predominantly due to the fact that the majority of the efficiency gains come in eliminating total internal reflection at the back face of the block. Even though the PMT only covers roughly 30% of the area of the back of the block focusing geometries proved not to be effective for the (divergent) Čerenkov photon angular distribution. The light

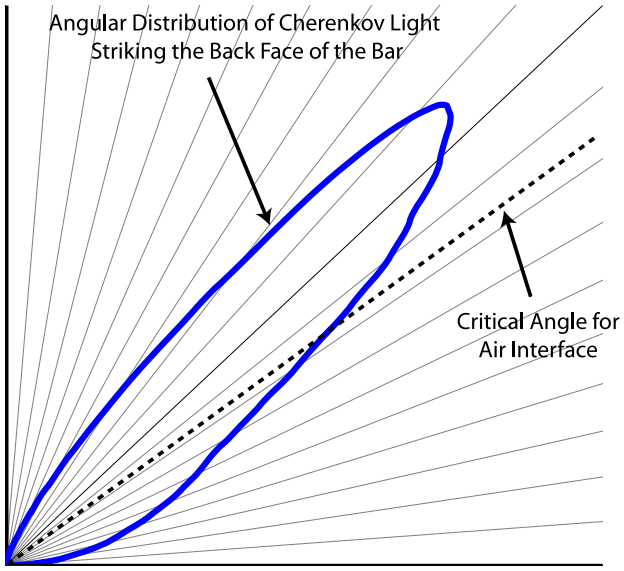

Figure 4.5: Simulated distribution of incident angle for Čerenkov photons produced by an incident 1 GeV photon. The critical angle for total internal reflection for a lead glass and air interface is shown.

guides will be cemented onto the PMT window. The joint between light guide and lead glass bar will be made with a clear silicon optical cookie which provides a stable optical joint that can easily be broken in case the PMT needs to be replaced or repaired. A sketch of the light guide design is shown in Figure 4.6.

Since Čerenkov photons, on average, tend to have a relatively high incident angle distribution, a variety of reflective coatings were considered to improve the efficiency of the light guide. Our bench test setup utilized fiber optic connections to inject blue light from an LED into a test lead glass bar at a variety of angles. This allowed us to effectively probe the light guide efficiency and compare with the same GEANT model of the setup discussed above. We tested cylindrical light guides of varying length with three types of surface treatments: (1) no coating or wrapping, (2) a vapor deposited aluminum coating, and (3) a loose aluminized mylar wrapping. In general we found that loose aluminized mylar wrappings, were most effective. The efficiency showed a mild dependence on length with a loss of roughly 4%/cm.

Magnetic shielding: As noted above, an essential function of the light guide, in addition to improving light collection of the PMT, is to allow the PMT photocathode to be recessed inside of a soft iron tube that shields strong solenoid fringe fields. In the GLUEX configuration the fringe field from the solenoid at the location of the PMT's is estimated to be about 200 Gauss. Based on tests using a 1-m diameter Helmholtz coil field, a soft iron tube of 4 cm outer diameter with a wall thickness of about 2.3 mm will shield a magnetic field along the axis of the tube from 200 Gauss down to 10-20 Gauss at a location of 4 cm (over one photocathode diameter) inside the tube [12] and then μ-metal shielding will further reduce the field to a sufficiently low level.

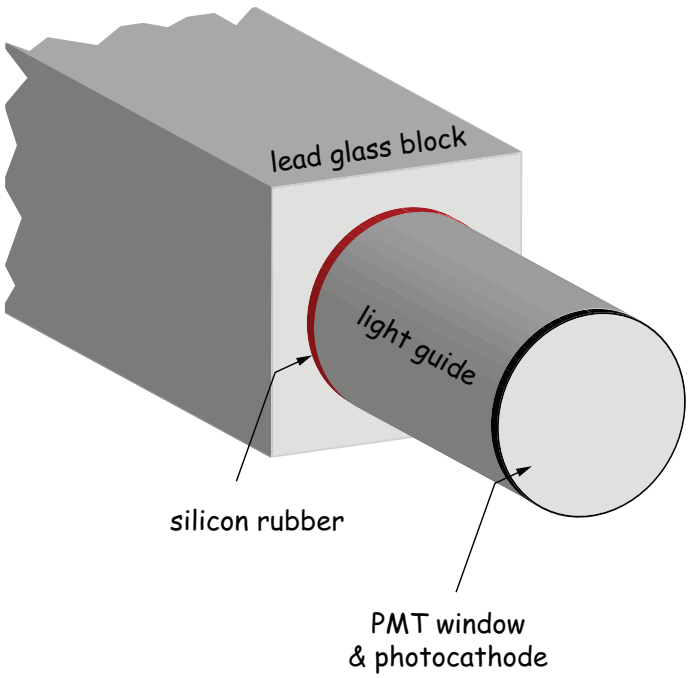

Figure 4.6: The PMT is glued to a light guide that couples to the lead glass with a silicon rubber cookie.

Projected performance characteristics: To summarize, we anticipate that eliminating light trapping by total internal reflection at the back of the block to provide an increase in transmission efficiency of roughly a factor of three. The light guide must be of sufficient length to adequately shield the PMT photocathode. Using an aluminized mylar wrapping the efficiency for a 4 to 5 cm light guide is expected to be roughly 80%, yielding roughly a factor of 2.5 gain in efficiency over E852 and RadPhi. MC simulations indicated that photo-statistics contribution to the $7.3\%/\sqrt{E(\mathrm{GeV})}$ statistical energy resolution term in RadPhi was 6.0%[3]. With the improved light coupling, we anticipate the photo-statics contribution to improve to 3.8% and the total statistical energy resolution to improve to $5.6\%/\sqrt{E(\mathrm{GeV})}$.

In addition to the improvement in energy resolution, there an equally important benefit in the sensitivity to low energy showers. Not only is the photon detection threshold improved, but blocks around the perimeter of a higher energy shower are more easily detected and therefore the resolution on these showers also improves. Figure 4.7 shows the ADC spectrum for events in which a cosmic ray passed transversely through a single lead glass block. One can clearly note the difference in gain between the two light couplings with the proposed wrapped cylindrical light guide giving roughly a factor of 2-3 gain in signal amplitude. Monte Carlo studies indicate that a cosmic ray passing transversely through the block generates roughly as many photoelectrons as a 30 MeV photon incident along the axis of the block. We therefore anticipate the low energy threshold for showers in the FCAL to be about 30 MeV.

[3]The remainder comes from fluctuations in Čerenkov light production and statistical losses in blocks surrounding the core of the shower.

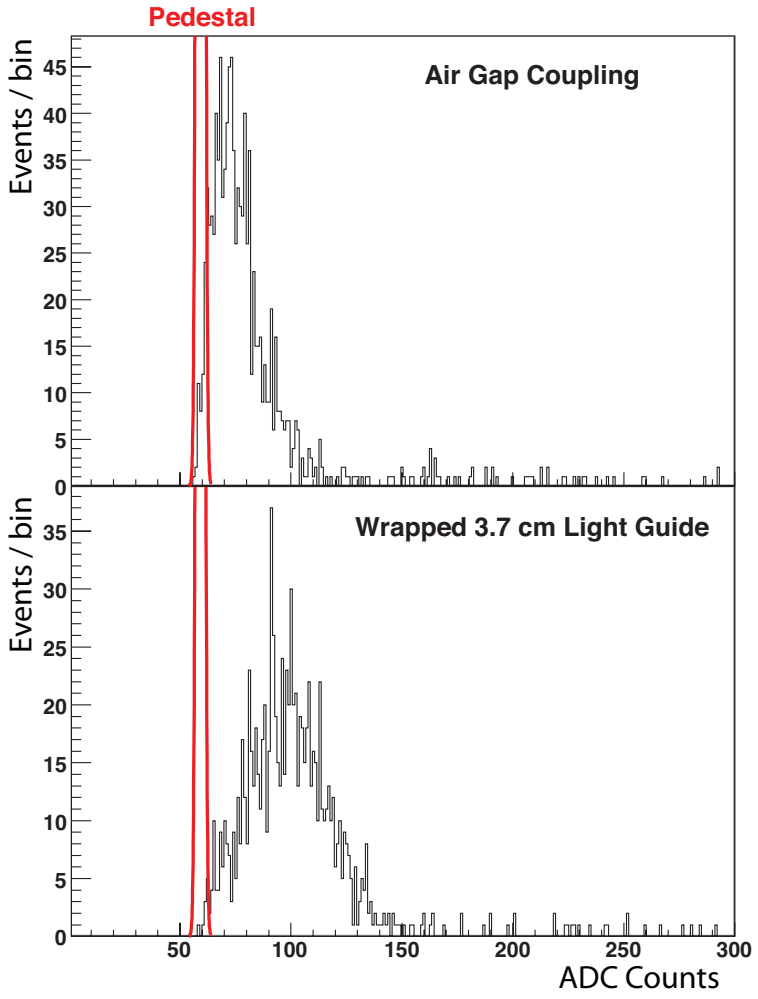

Figure 4.7: Raw ADC spectra from FEU 84-3 PMTs for cosmic rays passing transversely through a lead glass block. In the top plot there is a small (< 1 mm) air gap between the PMT and the lead glass block, while a 3.7 cm cylindrical light guide with aluminized mylar wrapping is used for the bottom plot.

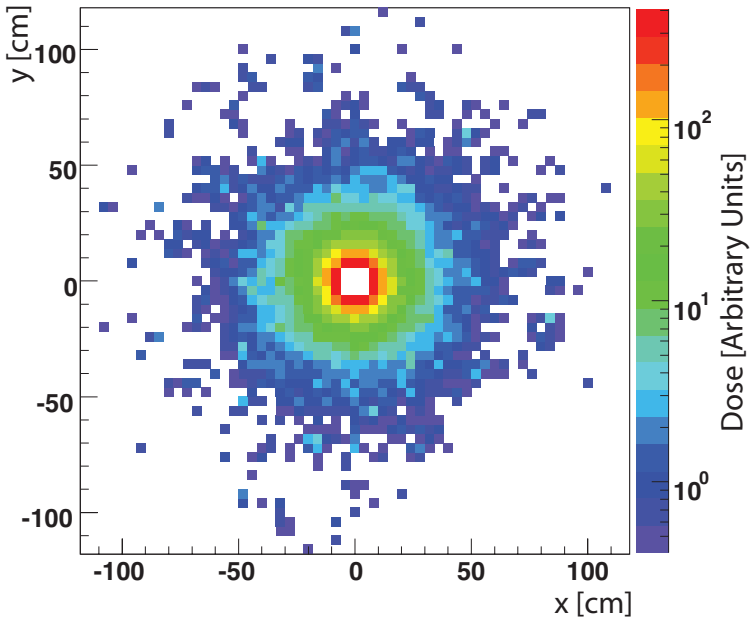

Figure 4.8: Expected distribution of radiation dose across the face of the FCAL. The size of each bin is equal to one block. The (logarithmic) vertical scale is total dose rate in arbitrary units.

4.4.2 Radiation damage mitigation

Earlier we discussed the evidence of radiation damage in the region near the beam hole in the RadPhi experiment. Our design addresses these issues by making use of radiation-hard (type F108) lead glass in the region surrounding the beam hole and allowing for in situ curing any radiation damage to the lead glass blocks (of type F8-00) surrounding the radiation-hard region.

Use of radiation-hard glass: Figure 4.2 shows the drop in gain for a type F8-00 block in the RadPhi environment next to the beam hole. It is expected that this radiation environment is within a factor of two of what is expected for the high rate running at GlueX. Figure 4.8 shows the expected distribution radiation dose rate across the face of the FCAL which the size of one bin is the size of a single block. The current plan is to instrument the inner 11×11 array with radiation-hard F108 glass. In the surrounding region the dose will be roughly an order of magnitude less, resulting in a drop in gain due to radiation damage of roughly 12% per 1000 hours of beam time (according to Figure 4.2).

Type F108 lead glass is a factor of 100 more radiation-hard than the type of glass used in E852 and RadPhi. We plan to instrument the inner layers around the beam hole with this glass. Figure 4.9 shows the transmission as a function of wavelength for a new lead glass bar of the type used in E852 and RadPhi, a bar of the same type that was damaged by radiation in RadPhi and for F101[4]. Figure 4.10 shows the relative photon yields for the RadPhi and F101 transmissions, convoluted with the expected Cerenkov light yield ($\propto 1/\lambda^2$) and the quantum efficiency of the FEU 84-3 [3] as a function of wavelength. The integrals of these curves for

[4]The data for the F101, which is expected to perform similarly to F108, were obtained from a plot in the talk by A. Vandenbrouke and C. Miller titled *Simulation of the HERMES Lead Glass Calorimeter Using a LUT* at the XII$^{\text{th}}$ International Conference on Calorimetry in High Energy Physics, Chicago, June 2006

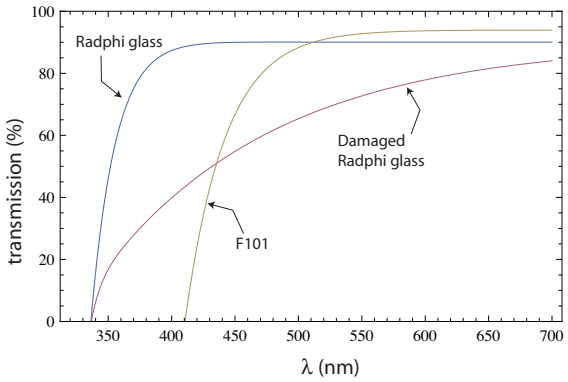

Figure 4.9: Transmission as a function of wavelength for a new lead glass bar of the type used in E852 and RadPhi, a bar of the same type that was damaged by radiation in RadPhi and for F101.

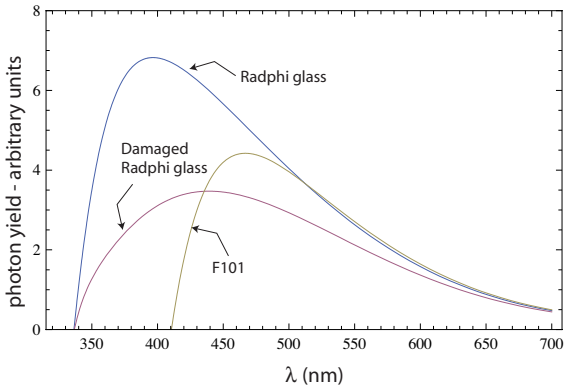

Figure 4.10: The relative photon yields for the the RadPhi and F101 transmissions, convolved with the expected Čerenkov light yield ($\propto 1/\lambda^2$) and the quantum efficiency. The integrals of these curves for the undamaged Raphi block to the damaged blocked to F101 are in the ratio of 1.0:0.60:0.55.

the undamaged RadPhi block to the damaged blocked to F101 are in the ratio of 1.0:0.60:0.55. While the use of radiation-hard glass will result in a factor of two loss of light initially, the transmission of these bars is expected remain relatively constant throughout the life of the experiment. Since type F108 (and F101) glass has a similar chemical composition to the F8-00 glass used in the remainder of the calorimeter we do not expect large deviations in the shape of electromagnetic showers that border on the boundary between two types of glass. It is anticipated that our reconstruction code need only account for the differing gain between the two types of blocks.

In situ UV curing: As noted above, the type F8-00 blocks surrounding the radiation-hard center of the calorimeter may experience some radiation damage at the level of $\approx 10\%$ reduction Radiation damage in lead glass is known to be temporary and to largely heal itself on the time scale of a few months. The healing can be accelerated by the use of ultraviolet (UV) light. This approach was adopted for the most affected blocks in the RadPhi experiment. During an extended down-time in the run, the PMT and base for selected blocks were removed and a UV light guide attached to a quartz-envelope mercury vapor lamp was inserted [13]. The

output of the lamp was 5 W/cm^2 in the range 300-480 nm, with a peak intensity at 365 nm. The affected blocks were each illuminated for periods of 6-8 hours. These blocks showed a gain increase of 30% following this treatment, nearly recovering their initial performance. Depending on actual dose, it is possible that a similar UV curing may be needed for type F8-00 blocks outside of the radiation-hard region of the GlueX detector. The glass support structure and surrounding equipment is being designed to permit access the the upstream face of lead glass wall to allow effective UV curing if needed.

4.5 GlueX Electronics

4.5.1 Cockcroft-Walton PMT bases

The Cockcroft-Walton (CW) base design described in reference [1] was modified somewhat for GlueX and 100 prototype bases were constructed. In the new design, the supply voltage of 24 V is boosted up to 175 Volts by an inductive boost circuit. The 175 Volts feeds a diode-capacitor Cockcroft-Walton multiplier which provides cathode and dynode PMT bias voltages directly. An 80C51 series processor chip enables and disables the multipliers and handles communication via a CAN bus. The chip also includes eight ADCs, four of which which are used to monitor various voltages in the base. Temperature and current monitoring could be added with the spare ADC channels. While the current design uses CAN-bus for communication, other options are possible if desired.

The temperature stability of this base has been tested and compared to conventional resistor based voltage dividers [14]. No temperature dependence was found within the accuracy of the measurement by monitoring the gain stability. The gain is found to be stable on the order of 0.1%/°C. Long term operational tests have also been performed and no indications of base failure were observed.

The use of CW PMT bases has many advantages over conventional resistor bases. The most notable difference is power consumption and consequently generated heat. When operating normally the CW bases consume less than 200 mW of power per base. Since high voltage is generated directly on the base, the design eliminates the need for an 2800-channel high voltage distribution system resulting in not only reduced cost but also improved safety.

4.5.2 Flash ADC readout

The analog signal from the PMT is digitized with a newly developed flash analog to digital converter (fADC) from JLAB. This fADC has a sampling frequency of 250 MHz (4 ns period) and samples a resolution of 12 bits. Studies have shown that the error on the integrated pulse is insignificant compared with the energy resolution at this sampling frequency and depth [15]. The buffer size covers a 3.6 μs time window. Upon receiving a trigger the fADC will process a portion of the buffer and return the integrated charge and time of each pulse in the buffer. The memory on the fADC is dual-ported so the system operates with zero dead-time, a design requirement for all GlueX data acquisition electronics.

The fADC provides some information on arrival the time of FCAL PMT pulses that is important for suppressing the large electromagnetic backgrounds in the experiment. The path length difference in photons from the target is insignificant and the production of Čerenkov light in the block is very fast. An "offline" examination of the distribution of pulse times for each of the recorded blocks provides important informa-

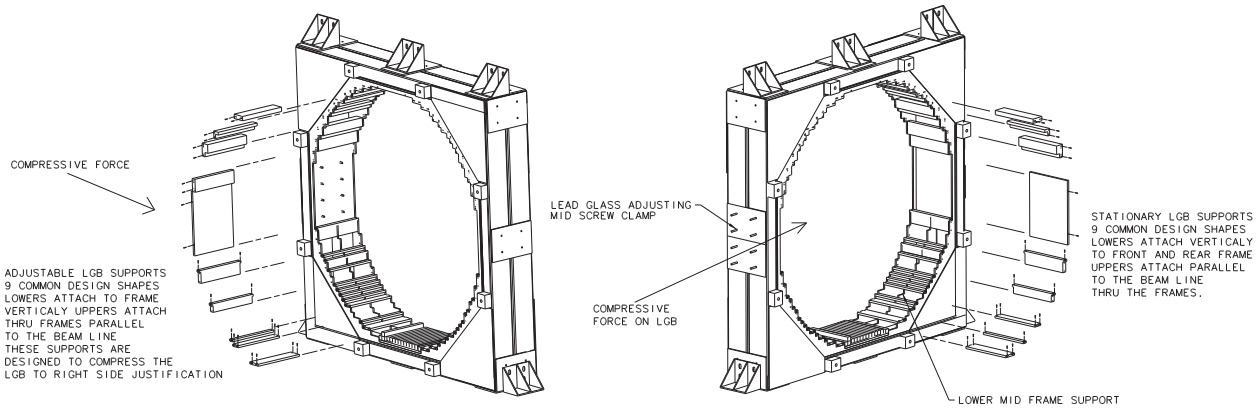

Figure 4.11: A sketch of the glass support structure.

tion. First, outliers from the core average pulse time are characteristic of electromagnetic backgrounds from neighboring beam bunches and can be discarded. Second, a precise determination of the event time can be obtained by the average pulse time. In all-neutral events, this event time is important for selecting the tagger hit from the electron that radiated the beam photon.

In addition, the FCAL fADCs serve as an input to the trigger. A running sum of all fADC channels will be computed by an "energy sum" board in each crated and relayed to the trigger processor. This information is critical for forming a trigger for events in which the majority of the produced particles are neutral.

4.6 Mechanical support and construction considerations

The holding structure of the forward calorimeter is divided into two main parts: an upstream glass support structure to hold the lead glass blocks and a downstream wall to hold the PMTs and bases. The entire structure is enclosed in a light tight covering. A dark room downstream behind the PMT holding structure provides access to PMT bases and allows one to easily service the detector electronics while maintaining a dark environment.

4.6.1 Lead glass holding structure

The mechanical challenge of the glass holding structure is that it must support a circular array in such a way that gaps between blocks are eliminated. A sketch of this holding structure, manufactured from aluminum, appears in Figure 4.11. It will allow the stacking of lead glass blocks row by row from the bottom. Each row can be adjusted, shimmed and clamped horizontally. Horizontal bolts will be used to apply pressure to shimming plates that will clamp the lead glass blocks in rows of the same width. The wall as a whole will be adjustable in height as well roll and pitch. The stacking of the blocks will be done in such a way that the down stream faces of all blocks will form one smooth surface onto which the PMTs will couple.

4.6.2 PMT cellular wall

The "cellular wall" provides a rigid assembly for attaching the PMTs to each of the blocks. The design illustrated in Figure 4.12 is based largely off of the design used for E852 and RadPhi experiments. The structure consists of individual soft iron tubes that are held together by a 1" aluminum front and back plate. The plates have drilled holes into which the soft iron tubes are press-fit. The space between the iron tubes and the two aluminum plates is filled with epoxy to make the wall mechanically rigid. This structure is then mounted at the back of the lead glass support. PMTs with their bases are loaded into each tube, which also serves as a magnetic shield, from the back and pressed up against the lead glass block to establish an optical coupling using silicon rubber cookies as noted above and in Figure 4.6. Sufficient pressure of ≤ 1 psi to preserve the optical joint is maintained by spring loaded screws that fasten the PMT base to the back plate of the cellular wall.

4.7 Summary

We have presented a design for the GlueX forward calorimeter that is largely based off of experience from similar lead glass calorimeters used for the E852 and RadPhi experiments. The design improves the optical coupling between lead glass bars and PMTs resulting in notable resolution gains and improved sensitivity to low energy showers. We plan to utilize a combination of radiation-hard blocks and in situ UV curing to handle the intense radiation environment around the beam. Readout will be achieved by utilizing a flash ADC digitization and trigger scheme that results in zero dead-time and provides both time and energy information for each block as need to reconstruct showers and minimize electromagnetic backgrounds from neighboring events. The anticipated performance of this detector for a variety of physics channels is discussed in detail in the next chapter.

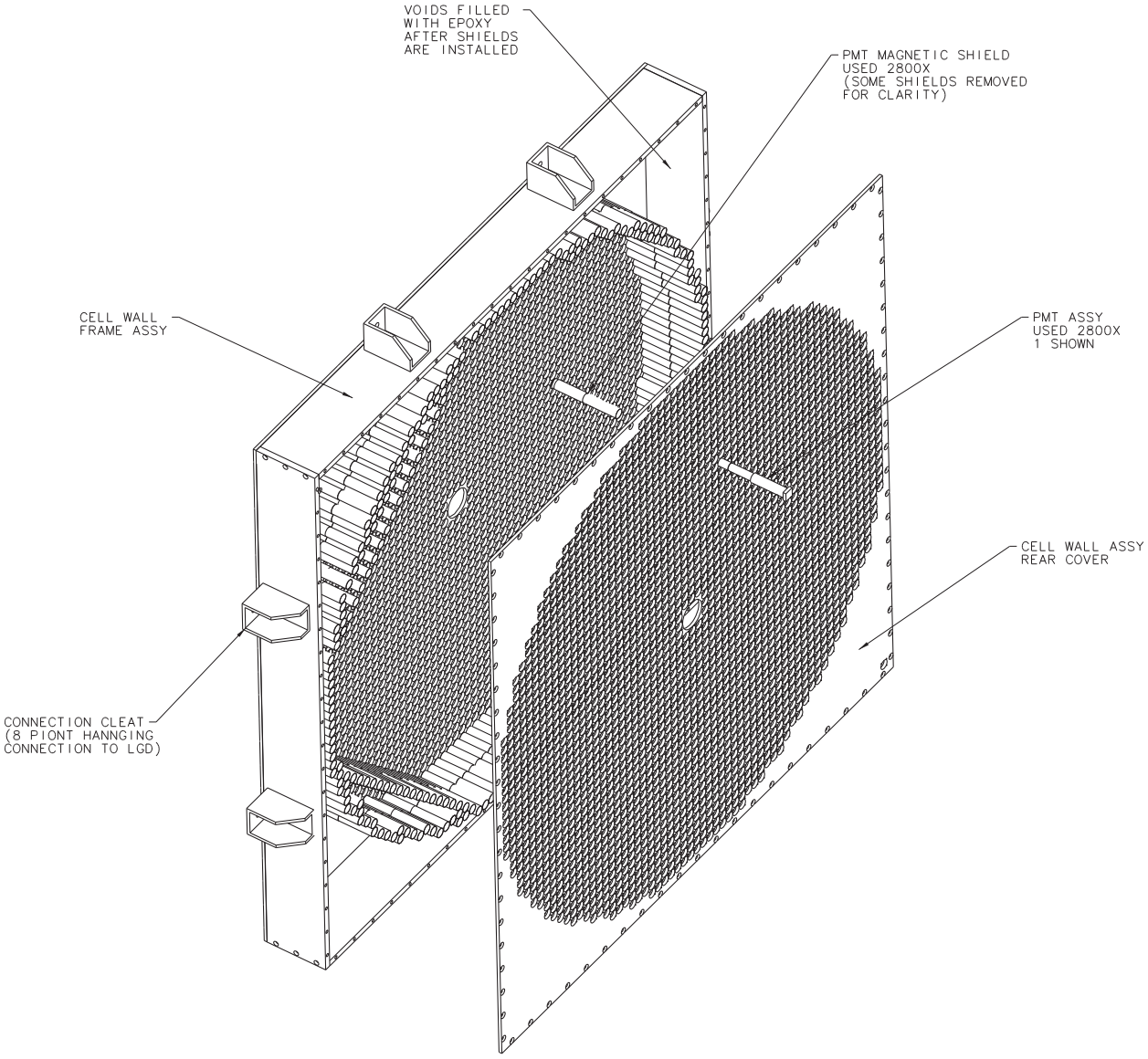

Figure 4.12: A sketch of the PMT cell wall.

References

[1] A. Brunner et al. A Cockcroft-Walton base for the FEU84-3 photomultiplier tube. *Nucl. Instrum. Meth.*, A414:466–476, 1998.

[2] A. Dzierba. Overview of the BNL E852 Experiment. Technical report, GlueX Collaboration, 2007. GlueX-doc-873-v1.

[3] B. B. Brabson et al. A study of two prototype lead glass electromagnetic calorimeters. *Nucl. Instrum. Meth.*, A332:419–443, 1993.

[4] R. R. Crittenden et al. A 3000 element lead-glass electromagnetic calorimeter. *Nucl. Instrum. Meth.*, A387:377–394, 1997.

[5] J. Gunter et al. A partial wave analysis of the $\pi^0\pi^0$ system produced in $\pi^- p$ charge exchange collisions. *Phys. Rev.*, D64:072003, 2001.

[6] A. R. Dzierba et al. A study of the $\eta\pi^0$ spectrum and search for a $J^{PC} = 1^{-+}$ exotic meson. *Phys. Rev.*, D67:094015, 2003.

[7] A. R. Dzierba et al. A partial wave analysis of the $\pi^-\pi^-\pi^+$ and $\pi^-\pi^0\pi^0$ systems and the search for a $J^{PC} = 1^{-+}$ meson. *Phys. Rev.*, D73:072001, 2006.

[8] P. Eugenio. A study of the $\omega\eta$ system produced in the reaction $\pi^- p \to \pi^+\pi^- 4\gamma n$ at 18 GeV/c. *Nucl. Phys.*, A675:241c–244c, 2000.

[9] P. Eugenio and P. Randerson. A study of the $\eta\eta\pi^-$ and $\omega\eta\pi^-$ systems produced in the reaction $\pi^- p \to p\pi^+\pi^-\pi^- 4\gamma$ at 18 GeV/c. *Nucl. Phys.*, A675:245c–248c, 2000.

[10] R. T. Jones et al. A bootstrap method for gain calibration and resolution determination of a lead-glass calorimeter. *Nucl. Instrum. Meth.*, A566:366–374, 2006.

[11] C. Cude, M. Shepherd, R. Mitchell, and S. Teige. Optimization of the GlueX FCAL light guide design. Technical report, GlueX Collaboration, 2007. GlueX-doc-850-v1.

[12] S. Denisov et al. Studies of magnetic shielding for phototubes. *Nucl. Instrum. Meth.*, A533:467–474, 2004.

[13] R. T. Jones et al. Performance of the RADPHI detector and trigger in a high rate tagged photon beam. *Nucl. Instrum. Meth.*, A570:384–398, 2007.

[14] J. Dickey, E. Scott, M. Shepherd, P. Smith, and S.Teige. Temperature dependence of FEU84-3 PMT's and IU Cockcroft-Walton bases. Technical report, GlueX Collaboration, 2006. GlueX-doc-657-v1.

[15] M. Shepherd. Flash ADC simulations for Hall D. Technical report, GlueX Collaboration, 2000. GlueX-doc-424-v1.